Cellular/Molecular

Long-Term Potentiation-Dependent Spine Enlargement Requires Synaptic Ca^{2+}-Permeable AMPA Receptors Recruited by CaM-Kinase I

Dale A. Fortin, Monika A. Davare, Taasin Srivastava, James D. Brady, Sean Nygaard, Victor A. Derkach, and Thomas R. Soderling

Vollum Institute, Oregon Health and Science University, Portland, Oregon 97239

It is well established that long-term potentiation (LTP), a paradigm for learning and memory, results in a stable enlargement of potentiated spines associated with recruitment of additional GluA1-containing AMPA receptors (AMPARs). Although regulation of the actin cytoskeleton is involved, the detailed signaling mechanisms responsible for this spine expansion are unclear. Here, we used cultured mature hippocampal neurons stimulated with a glycine-induced, synapse-specific form of chemical LTP (GI-LTP). We report that the stable structural plasticity (i.e., spine head enlargement and spine length shortening) that accompanies GI-LTP was blocked by inhibitors of NMDA receptors (NMDARs; APV) or CaM-kinase kinase (STO-609), the upstream activator of CaM-kinase I (CaMKI), as well as by transfection with dominant-negative (dn) CaMKI but not dnCaMKIV. Recruitment of GluA1 to the spine surface occurred after GI-LTP and was mimicked by transfection with constitutively active CaMKI. Spine enlargement induced by transfection of GluA1 was associated with synaptic recruitment of Ca^{2+}-permeable AMPARs (CP-AMPARs) as assessed by an increase in the rectification index of miniature EPSCs (mEPSCs) and their sensitivity to IEM-1460, a selective antagonist of CP-AMPARs. Furthermore, the increase in spine size and mEPSC amplitude resulting from GI-LTP itself was blocked by IEM-1460, demonstrating involvement of CP-AMPARs. Downstream signaling effectors of CP-AMPARs, identified by suppression of their activation by IEM-1460, included the Rac/PAK/LIM-kinase pathway that regulates spine actin dynamics. Together, our results suggest that synaptic recruitment of CP-AMPARs via CaMKI may provide a mechanistic link between NMDAR activation in LTP and regulation of a signaling pathway that drives spine enlargement via actin polymerization.

Introduction

Dendritic spines are highly dynamic structures that receive the vast majority of excitatory synaptic input within the brain. A long-held hypothesis states that functional changes in synaptic efficacy accompany changes in synapse/spine morphology (Ramón y Cajal, 1911; Hebb, 1949). Particularly, changes in spine structure and number have been associated with long-term potentiation (LTP) (for review, see Carlisle and Kennedy, 2005; Tada and Sheng, 2006; Bourne and Harris, 2008), a candidate cellular model for learning and memory. Indeed, several types of mental retardation and cognitive dysfunction are associated with abnormalities in spine density and morphology (Purpura, 1974; Kaufmann and Moser, 2000; Fiala et al., 2002).

Alterations in spine morphology are tightly coupled to changes in filamentous actin present throughout the spine (Fifkova and Delay, 1982; Matus et al., 1982; Matsuzaki et al., 2004) where it also anchors many postsynaptic channels and signaling proteins (Oertner and Matus, 2005). Spine actin is modulated largely by Rac1-activated PAK that activates LIM-kinase (LIMK) (for review, see Boda et al., 2006) to promote actin polymerization by phosphorylating actin-depolymerizing factor/cofilin, thereby inhibiting actin depolymerizing activity (Bamburg et al., 1999). Activated PAK1 and PAK3 are concentrated in dendritic spines (Penzes et al., 2003; Hayashi et al., 2004), and genetic disruption (Allen et al., 1998) or small peptide inhibitors of PAK result in altered spine phenotype and impaired memory consolidation (Hayashi et al., 2004), whereas constitutively active (ca) PAK promotes spine formation (Hayashi et al., 2007). $LIMK^{-/-}$ mice show reduced levels of phosphorylated cofilin, abnormal spine morphology, and deficits in activity-dependent synaptic plasticity and spatial learning (Meng et al., 2002), consistent with the role of LIMK in stabilizing F-actin in spines. Notably, genetic mutations of PAK-3 and LIMK-1 have been implicated in nonsyndromic X-linked mental retardation (Allen et al., 1998) and Williams syndrome (Tassabehji et al., 1996), respectively.

Prior work establishes that actin-mediated spine enlargement associated with LTP requires increased intracellular calcium (Fifkova, 1985; Oertner and Matus, 2005; Vlachos et al., 2009). It has been assumed that the major source of this calcium is due to activity-dependent activation of NMDA receptors (NMDARs). However, we and others have recently shown that LTP induced by certain protocols (e.g., theta-burst) is associated with the transient incorporation of calcium-permeable AMPA receptors (CP-

Received April 6, 2010; revised June 21, 2010; accepted July 12, 2010.

This work was supported by National Institutes of Health Grant NS027037 (T.R.S.).

Correspondence should be addressed to Thomas R. Soderling, 3181 SW Sam Jackson Park Road, Portland, OR 97239. E-mail: soderlit@ohsu.edu.

DOI:10.1523/JNEUROSCI.1746-10.2010

 0270-6474/10/3011565-11$15.00/0

AMPARs) into the synapse (Plant et al., 2006) (but, see also Adesnik and Nicoll, 2007; Gray et al., 2007; Lu et al., 2007; Guire et al., 2008). We found that synaptic incorporation of CP-AMPARs, which can significantly enhance synaptic conductance, requires the activation of CaMKinase I (CaMKI) (Guire et al., 2008), but a role for CP-AMPARs in structural plasticity of spines has not previously been reported. We previously demonstrated that spinogenesis during early development requires CaMK1-mediated phosphorylation of βPIX to activate Rac1 (Saneyoshi et al., 2008).

Here, we have demonstrated that synaptic recruitment of CP-AMPARs by CaMKI contributes to actin-dependent structural plasticity induced by glycine-induced LTP (GI-LTP). We also show that synaptic CP-AMPARs are essential for downstream activation of the Rac/PAK/LIMK pathway necessary for actin-mediated spine enlargement and associated synaptic potentiation.

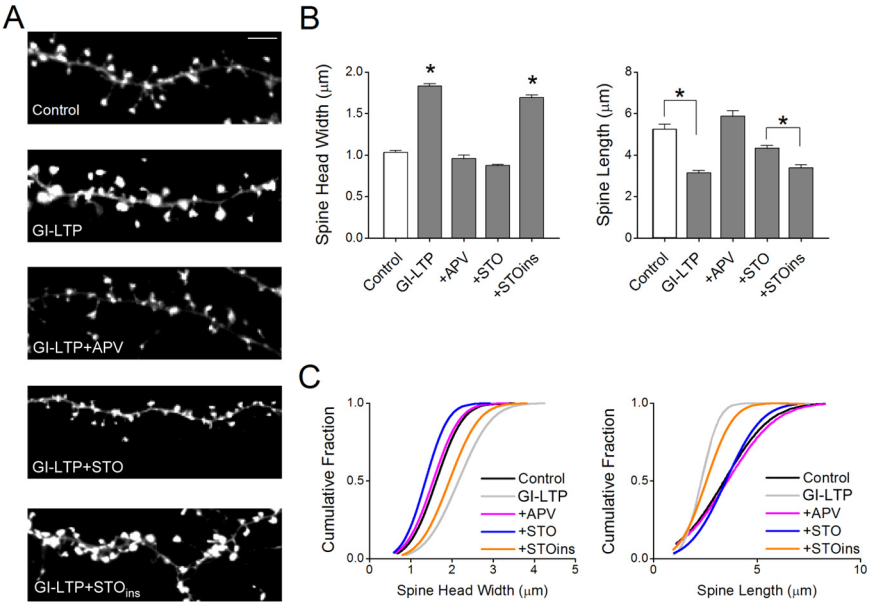

Figure 1. GI-LTP structural plasticity requires NMDARs and CaMKK. ***A***, Representative fluorescence images of secondary hippocampal dendritic spines visualized using mRFP-β-actin for conditions indicated. For some experiments, neurons were pretreated with either APV (50 μM, 30 min) or STO-609 (10 μM, 4 h) or transfected with plasmid expressing a STO-insensitive mutant of CaMKK (STOins, 24 h) before GI-LTP treatment (10 min GI-LTP) (see Materials and Methods). Scale bar, 5 μM. ***B***, Quantitative analysis of spine head width (left) and spine length (right) for conditions indicated. ***C***, Cumulative distribution plots for spine head width (left) and length (right) of the population of spines analyzed ($n = 75–100$ spines/neuron; 5–6 neurons per coverslip). Error bars indicate SEM ($n = 8–10$ coverslips per condition from 2–3 independent cultures). *$p < 0.05$ by Student's *t* test.

Materials and Methods

Reagents and constructs. D-(−)-2-Amino-5-phosphonopentanoic acid (D-APV); 1,8-Naphthoylene benzimidazole-3-carboxylic acid (STO-609); *N*,*N*,*N*,-trimethyl-5-[(tricyclo[3.3.1.13,7]dec-1-ylmethyl) amino]-1-pentanaminiumbromide hydrobromide (IEM-1460); [*R*-(*R**,*S**)]-5-(6,8-dihydro-8-oxofuro[3,4-e]-1,3-benzodioxol-6-yl)-5,6,7,8-tetrahydro-6,6-dimethyl-1,3-dioxolo[4,5-g] isoquinolinium iodide (bicuculline methiodide); strychnidin-10-one hydrochloride (Strychnine); 6-cyano-7-nitroquinoxaline-2,3-dione disodium (CNQX); and octahydro-12-(hydroxymethyl)-2-imino-5,9:7,10a-dimethan-o-10aH-[1,3]dioxocino [6,5-d]pyrimidine-4,7,10,11,12-pentol (TTx) were purchased from Tocris Bioscience. Latrunculin A was purchased from Calbiochem.

caCaMKI, dominant-negative (dn) CaMKI, dnCaMKK, $CaMKK_{ins}$, monomeric red fluorescent protein (mRFP)-β-actin, dnPAK1, and myc-tagged Rac1 (Rac1) have been described previously (Wayman et al., 2004, 2006; Saneyoshi et al., 2008; Impey et al., 2010).

Cell culture and neuronal transfection. Hippocampal neurons were isolated from postnatal day 0–2 Sprague Dawley rats, as described previously (Wayman et al., 2006). After harvesting, neurons were plated on poly-L-lysine-coated (Sigma; molecular weight, 30 kDa) 12 mm glass coverslips at a density of 4.0×10^4 cells per square centimeter or coated plastic 35 mm wells at 4.5×10^5 cells per square centimeter. Neurons were maintained in Neurobasal A media (Invitrogen) supplemented with B27 (Invitrogen) and 0.5 mM L-glutamine with 5 μM cytosine-D-arabinofuranoside added at 2 d *in vitro* (DIV). Neurons were cultured for 13–16 d before being transfected using LipofectAMINE 2000 (Invitrogen) and/or treated with indicated pharmacological reagents. DNA, transfection reagent, and transfection duration were optimized to minimize toxicity and maximize transfection efficiency (0.5–3% of neurons between 13 and 16 DIV).

Quantification of spine density and morphology. For experiments used in the quantification of spine morphology, hippocampal neurons were first transfected with mRFP-β-actin between 12 and 14 DIV to aid in the visualization of dendritic spines (Saneyoshi et al., 2008) with or without test plasmids. Expression of low levels of β-actin has been shown to have no significant effect on either spine density or size (Saneyoshi et al., 2008). Before imaging, neurons were fixed for 15 min at room temperature in prewarmed (37°C) fixative (4% paraformaldehyde, 4% sucrose in PBS). Fluorescent images were acquired using a cooled CCD camera (Hamamatsu Photonics) attached to a Carl Zeiss Axiplan2 inverted microscope with a 63× oil-immersion lens. Morphometric measurements of spine head area, length, head width, and density were performed using National Institutes of Health Image J software (Abramoff et al., 2004). Spines were defined as having head widths that were at least twice the diameter of the spine neck. Three 50 μm sections of secondary dendrite from each neuron were analyzed. The number of spines and coverslips quantified for each experiment is reported within the corresponding figure legend. Each experiment was repeated at least three times with independent culture preparations.

Immunocytochemistry. Hippocampal neurons were fixed in 4% paraformaldehyde, 4% sucrose in PBS, and 50 mM HEPES, pH 7.5, at 37°C for 15 min. Neurons were rinsed three times for 10 min in PBS and blocked for 1 h in blocking buffer (PBS containing 3% BSA) at room temperature (22°C). Neurons were then stained for surface-expressed GluA1 using a rabbit anti-GluA1 N-terminal antibody (Calbiochem, 1:100), which recognizes amino acids 271–285 of rat GluA1, in blocking buffer overnight at room temperature and washed three times for 10 min in blocking buffer. Surface GluA1 was subsequently detected by incubating coverslips in blocking buffer containing anti-rabbit Alexa Fluor-488 (Invitrogen, 1:2000) for 40 min at room temperature. Hoechst dye (Molecular Probes) was also added to the secondary buffer to allow assessment of cell viability. Coverslips were then washed quickly in PBS and mounted onto slides using Elvanol mounting medium.

GluA1 surface biotinylation. Biotinylation experiments were performed as previously described (Oh et al., 2006). Briefly, after treatments neuronal cell cultures were washed with cold artificial CSF (ACSF), pH adjusted to 8.2, to fully protonate amine groups before biotinylation. After removing the wash buffer cells were incubated with ice-cold ACSF, pH 8.2, containing 0.8 mg/ml NHS-SS-biotin (Soltec Ventures) for 30 min on a shaker at 4°C. Cells were then quenched with ACSF containing 50 mM Tris-HCl for 10 min on a shaker at 4°C. Cells were then flash frozen using liquid nitrogen and stored at −80°C before being subjected to an avidin pulldown.

For avidin pulldowns, cells were thawed on ice and lysed in ice-cold radioimmunoprecipitation assay lysis buffer. Lysates were then centrifuged for 10 min at 14,000 × *g* at 4°C to pellet insoluble material. Neu-

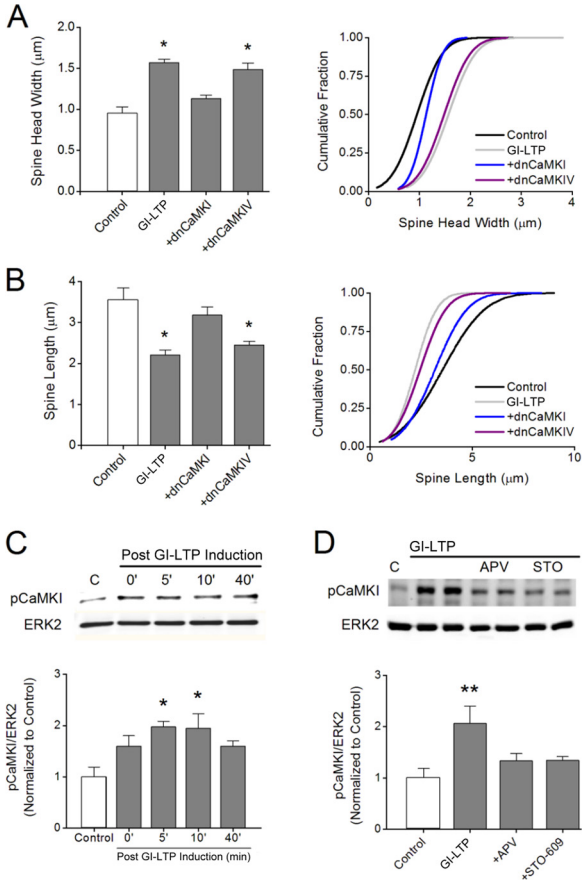

Figure 2. CaMKK signals through CaMKI but not CaMKIV to induce GI-LTP structural plasticity. ***A***, ***B***, Quantitative analysis (left) and cumulative distribution plots (right) for spine head width (***A***) and spine length (***B***) for each condition shown. Neurons were transfected with plasmids expressing dnCaMKI or dnCaMKIV 48 h before GI-LTP induction. $*p < 0.05$ by Student's *t* test. ***C***, Top, Representative Western blots for pCaMKI and total ERK2 (loading control) for the indicated time points after the 10 min GI-LTP treatment. Bottom, Quantification of pCaMKI intensities before and after GI-LTP ($n = 3$ independent experiments). Error bars indicate SEM ($n = 3$ from 3 independent experiments). $*p < 0.05$ by one-way ANOVA. ***D***, Top, Representative Western blots of pCaMKI and total ERK2 5 min after GI-LTP induction with or without APV or STO-609 (STO) treatments as in Figure 1. Bottom, Quantification of pCaMKI intensities for each condition shown ($n = 3$–5 from 3 independent experiments). Group data shown as mean ± SEM. $**p < 0.01$ by Student's *t* test.

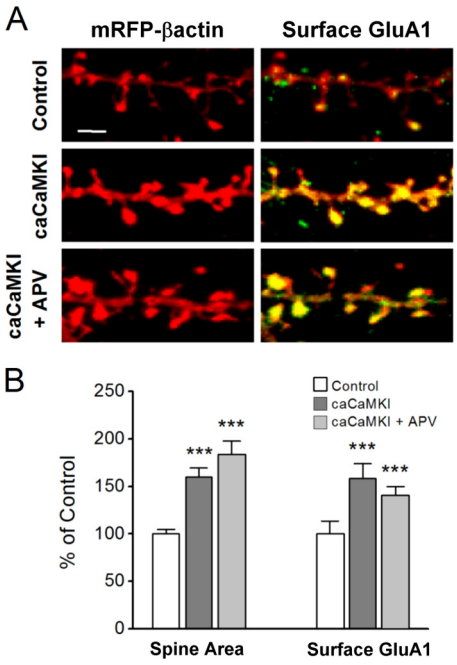

Figure 3. Constitutively active CaMKI mimics structural plasticity induced by GI-LTP and increases surface GluA1. ***A***, Immunofluorescence images of hippocampal dendritic spines highlighted with mRFP-β-actin (left) or superimposed with surface GluA1 pseudo-colored in green (right) for controls (top) or neurons transfected with caCaMKI (24 h before fixation) without (middle) or with (bottom) treatment with APV added immediately after transfection and kept present until fixation. Surface GluA1 staining was performed using an N-terminal antibody under nonpermeabilizing conditions. Scale bar, 2.5 μm. ***B***, Group data for spine head width and surface GluA1 for conditions illustrated in A ($n = 50$–75 spines per neuron; 5–8 neurons per coverslip). Error bars indicate SEM ($n = 8$ coverslips per condition from 3 independent cultures). $***p < 0.001$ by Student's *t* test.

travidin beads (20 μl, Pierce) were added to the supernatant. Lysates containing avidin beads were rotated at 4°C for 2 h and then washed two times with ice-cold lysis buffer. Biotinylated proteins were extracted with 2× SDS sample buffer supplemented with 50 mM DTT for 30 min at 50°C before being subjected to a Western blot. Western blotting was performed as previously described (Davare et al., 2004). Biotinylated GluA1 and total GluA1 (cell lysate) were probed with αGluA1 (courtesy of Dr. Wenthold, National Institutes of Health, National Institute on Deafness and Other Communication Disorders, Bethesda, MD) and detected with IR700- and/or IR800-conjugated secondary antibodies. Blots were quantified using software supplied with the Odyssey Infrared System (LI-COR Biosciences).

GST-PAK-PBD pulldowns. Hippocampal neurons were rapidly harvested with ice-cold PAK-PBD lysis buffer containing 1% Triton X-100, and (in mM) 50 HEPES, pH 7.4, 150 NaCl, and 25 $MgCl_2$ that was supplemented just before use with 1 mM DTT and protease and phosphatase inhibitors (leupeptin, aprotinin, benzamidine, pepstatin-A and antipain, cantharidic acid, and microcystin A). Cell lysates were centrifuged at 20,000 × *g* for 10 min to clear insoluble material. Cleared lysates were applied to preloaded glutathione Sepharose beads containing 30 μg of GST-PAK-PBD. Samples were incubated for 1–1.5 h on a rocker at 4°C. Resins were washed two times with cold lysis buffer and extracted with 2× SDS sample buffer. Activated endogenous Rac1 or transfected Myc-tagged Rac1 bound to PAK-PBD was detected by Western blotting with anti-Rac1 monoclonal antibody (BD Transduction, 1:1000) or 9E10 monoclonal anti-myc tag antibody (Developmental Studies Hybridoma Bank, 1:1000).

Electrophysiology. Whole-cell voltage-clamp recordings were performed on cultured hippocampal neurons, as described above, using an Axopatch-200b amplifier (Molecular Devices). Cells were continuously perfused (1 ml/min) with normal ACSF (nACSF) that contained the following (in mM): 125 NaCl, 2.5 KCl, 2 $CaCl_2$, 1 $MgCl_2$, 5 HEPES; and 33 glucose; pH was adjusted to 7.3 using NaOH. Osmolarity was adjusted to 290 mosmol/l. For isolating miniature EPSCs (mEPSCs), gabazine (10 μM), strychnine (3 μM), and tetrodotoxin (0.5 μM) were added to the external buffer to block $GABA_A$ receptor, glycine receptor, and Na channel activity, respectively. Patch electrodes were pulled from thin-walled borosilicate glass capillaries (tip resistance ranged from 4 to 6 MΩ) and filled with internal buffer solution that contained the following (in mM): 100 cesium methanesulfonate, 25 CsCl, 2 $MgCl_2$, 4 Mg^{2+}-ATP, 0.4 Na-GTP, 10 phosphocreatine, 0.4 EGTA, and 10 HEPES, pH 7.4 (284 mosmol/l). All experiments were performed at room temperature (22°C). Whole-cell recordings were only established after a high-resistance seal (> 2 GΩ) was achieved. Only cells that had an input resistance of > 150 MΩ and resting membrane potentials < −50 mV were considered for experiments. Resting membrane potentials were measured immediately upon breaking into whole-cell mode by setting the current to 0 pA. Cells were then voltage-clamped at a holding potential of −70 mV, unless otherwise noted. LTP was induced by switching perfusate to ACSF containing the following (in mM): 125 NaCl, 2.5 KCl, 2 $CaCl_2$, 5 HEPES, 33 glucose, 0.2 glycine, 0.02 bicuculline, and 0.003 strychnine for 10 min at room temperature before returning back to nACSF. Access resistance (R_a) was monitored at the beginning and end of each experiment with small voltage pulses, which typically ranged be-

tween 10 and 15 MΩ and were not compensated. Cells were rejected from analysis if R_a increased by >15% during the course of the experiment or if the input resistance fell below 150 MΩ.

Results

CaMKK is required for NMDAR-dependent structural plasticity of hippocampal dendritic spines

Recent evidence from cultured hippocampal neurons suggests formation of spines and synapses in early development is enhanced by CaMKK and CaMKI signaling downstream of NMDARs (Saneyoshi et al., 2008). In this study, we examined whether structural plasticity in mature cultured neurons (14–21 DIV), specifically, the persistent (> 30 min) spine expansion accompanying NMDAR-dependent LTP, also requires CaMKK/CaMKI signaling. This stable component of spine expansion, in contrast to the transient and larger initial spine enlargement, has been shown to be inhibited by the general CaMK inhibitors, KN-62 (Matsuzaki et al., 2004) and KN-93 (Steiner et al., 2008). To better define the role of CaMKs, we used a highly selective CaMKK inhibitor, STO-609 (Tokumitsu et al., 2002). STO-609 potently inhibits CaMKK at 5–10 μM with little or no effect on CaMKI, CaMKIV, CaMKII, PKA, PKC, or Erk1 (Tokumitsu et al., 2002, 2003). For example, in theta-burst LTP STO-609 blocks activation of CaMKI by CaMKK with no effect on CaMKII activation or its phosphorylation of GluA1 (Ser831) (Schmitt et al., 2005). In this case, synaptic potentiation itself is suppressed ~50%, indicating a potential role of CaMKK/CaMKI in theta-burst LTP (Schmitt et al., 2005; Guire et al., 2008).

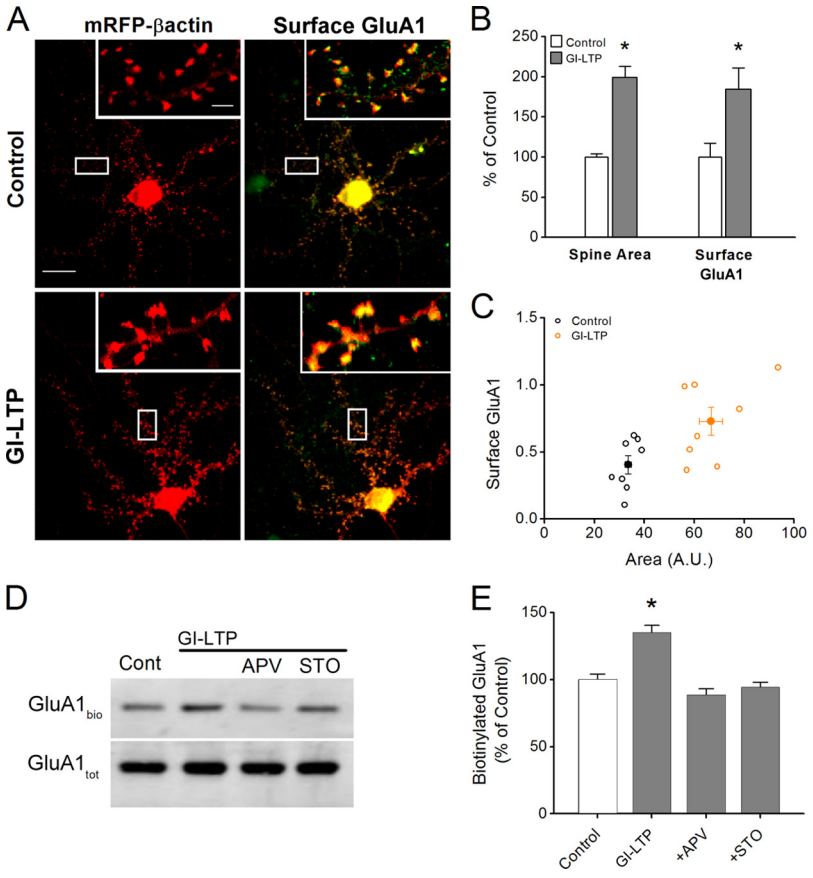

Figure 4. GI-LTP-induced surface trafficking of GluA1 requires CaMKK. ***A***, Immunofluorescence images of hippocampal dendritic spines transfected with mRFP-β-actin (left) or superimposed with surface GluA1 pseudo-colored in green (right) for control and GI-LTP-treated neurons. Scale bar, 15 μm; inset, 2.5 μm. ***B***, Quantification of spine head area and surface GluA1 ($n = 75–100$ spines per neuron; 6–8 neurons per coverslip) for control and GI-LTP-treated neurons ($n = 8$ coverslips per condition from 2 independent cultures). ***C***, Scatter plot of surface GluA1 and spine head area for control and GI-LTP-treated coverslips. ***D***, Representative Western blots of biotinylated surface GluA1 ($GluA1_{bio}$) and total GluA1 ($GluA1_{tot}$) for conditions shown. ***E***, Quantification of the ratio of surface biotinylated to total GluA1 for each condition indicated ($n = 8$ from 5 independent experiments). For GI-LTP-treated cultures, neurons were fixed or biotinylated 40 min after GI-LTP. Error bars indicate SEM. *$p < 0.05$ by Student's *t* test.

We induced NMDAR-dependent synaptic plasticity in our hippocampal cultures using a chemical LTP (c-LTP) protocol. There are two major c-LTP protocols commonly used; treatment with forskolin/rolipram (Otmakhov et al., 2004) and GI-LTP (Shahi and Baudry, 1993; Lu et al., 2001)—both exhibit many features characteristic of CA1 stimulus-induced LTP. However, whereas the forskolin/rolipram treatment strongly activates protein kinase A (PKA) throughout the neuron, both pre- and postsynaptically, we chose to use GI-LTP because it specifically stimulates NMDARs only at synapses receiving spontaneous release of glutamate. Thus, GI-LTP should more closely mimic stimulus-induced synaptic potentiation (see supplemental Table 1, supplemental Fig. S1, available at www.jneurosci.org as supplemental material). Furthermore, GI-LTP is associated with an increase in mEPSC amplitude (Lu et al., 2001; Oh and Derkach, 2005) and NMDAR-dependent spine expansion (Park et al., 2006; Korkotian and Segal, 2007) and synapse formation (Ovtscharoff et al., 2008). Stimulus-inducted LTP in region CA1 requires autonomous CaMKII activity due to autophosphorylation of Thr286 (Silva et al., 1992), and GI-LTP also results in CaMKII autophosphorylation (Oh and Derkach, 2005). Moreover, infusion of CaMKIINtide, the active peptide derived from the specific CaMKII inhibitor protein CaMKIIN (Chang et al., 1998, 2001), via the recording electrode blocks synaptic potentiation by GI-LTP (supplemental Fig. S2, available at www.jneurosci.org as supplemental material). Furthermore, transfection of cultured neurons with CaMKIIN blocked the formation of constitutively active (i.e., Thr286 autophosphorylated) CaMKII that occurs in GI-LTP and suppressed spine head enlargement (supplemental Fig. S2, available at www.jneurosci.org as supplemental material). Thus, GI-LTP closely mimics stimulus-inducted LTP including a requirement for CaMKII activation.

To quantify changes in spine morphology, hippocampal neurons were transfected with mRFP-β-actin at least 24 h before inducing GI-LTP. As shown in Figure 1*A*, β-actin is highly enriched in spines, and expression of β-actin itself does not affect spine morphology (Saneyoshi et al., 2008). To isolate the persistent spine expansion of distal dendritic spines, neurons were fixed 40 min after the induction of GI-LTP, individual transfected neurons were imaged, and dendritic spine head widths and lengths were measured. GI-LTP induced a significant increase in spine head width (control = 1.03 ± −0.02 μm; GI-LTP = 1.42 ± 0.03 μm) and decrease in spine length (control = 5.25 ± 0.23 μm; GI-LTP = 3.15 ± 0.11 μm), consistent with the formation of mushroom-shaped spines that form synapses (Fig. 1*B*). More-

over, cumulative probability plots of spine head width and length indicate that the structural plasticity was not limited to a subset of spines (Fig. 1*C*). This alteration in spine morphology induced by GI-LTP was dependent upon NMDARs as it was prevented by application of the NMDAR antagonist APV (50 μM) (Fig. 1*B*,*C*). More importantly, spine head enlargement was completely suppressed whereas spine length shortening was partially blocked (~50%) by inhibition of CaMKK with STO-609 (10 μM). To further confirm the specificity of STO-609, we induced GI-LTP in neurons cotransfected with a mutant form of CaMKK (L233F) that is 100-fold less sensitive to inhibition by STO-609 (Tokumitsu et al., 2003). Expression of this STO-insensitive CaMKK mutant prevented the STO-dependent suppression of spine morphology after GI-LTP (Fig. 1). These results strongly implicate a role for CaMKK in NMDAR-dependent structural plasticity. In addition to inducing changes in spine morphology, GI-LTP also resulted in an increase in spine density (control = 8.3 ± 0.4 spines/25 μm; GI-LTP = 11.7 ± 0.5 spines/25 μm; $p < 0.05$ by Student's *t* test) that was prevented by pretreatment with APV or STO-609 (data not shown).

CaMKI but not CaMKIV is necessary for structural plasticity

CaMKI and CaMKIV are two well established CaMKK substrates that require phosphorylation of their activation loops for their full catalytic activity. CaMKII does not have an activation loop phosphorylation site and is not activated by CaMKK (Tokumitsu et al., 1995). In fact, there is no known cross talk between the CaMKK/CaMKI/CaMKIV cascade and CaMKII. Since inhibition of CaMKK with STO-609 blocks GI-LTP spine plasticity (Fig. 1), we determined whether CaMKI or CaMKIV plays a role downstream from CaMKK by expressing the dn forms (i.e., catalytically inactive) of each kinase. We found that expression of dnCaMKI, but not dnCaMKIV, inhibited the structural plasticity associated with GI-LTP (Fig. 2*A*,*B*). Expression of dnCaMKI also blocked the increase in spine density after GI-LTP. These data indicate that CaMKI is the relevant substrate downstream of CaMKK during GI-LTP. To further test this hypothesis we assayed for CaMKI activation after GI-LTP using a phospho-specific antibody directed against the CaMKK phosphorylation/activation site in CaMKI. As shown in Figure 2*C*, GI-LTP induced a rapid phosphorylation of CaMKI by CaMKK that remained elevated for up to 40 min post induction. The activation of CaMKI by GI-LTP was significant but modest (2-fold) compared with KCl stimulation which gave a 14-fold activation (supplemental Fig. S3, available at www.jneurosci.org as supplemental material). Thus, GI-LTP may represent a moderate LTP induction protocol. Activation of CaMKI by GI-LTP was also dependent upon NMDAR activation since treatment with APV suppressed its activation (Fig. 2*D*).

To determine whether expression of CaMKI is sufficient to drive structural changes in dendritic spines, we transfected neurons with a constitutively active form of CaMKI (caCaMKI). We also examined the increase in surface GluA1, which is known to traffic into spines after the induction of synaptic plasticity (Hayashi et al., 2000; Lu et al., 2001; Pickard et al., 2001; Shi et al., 2001). We previously demonstrated that active CaMKI infused into neurons enhances synaptic incorporation of CP-AMPARs that lack the GluA2 subunit (Guire et al., 2008). Surface GluA1 content was assessed by immunofluorescence microscopy using an N-terminal antibody under nonpermeabilizing conditions (see Materials and Methods). We found that expression of caCaMKI (24 h) in neurons increased both spine head area as well as surface GluA1 within spines (Fig. 3). These increases were also observed in the presence of APV as would be expected since

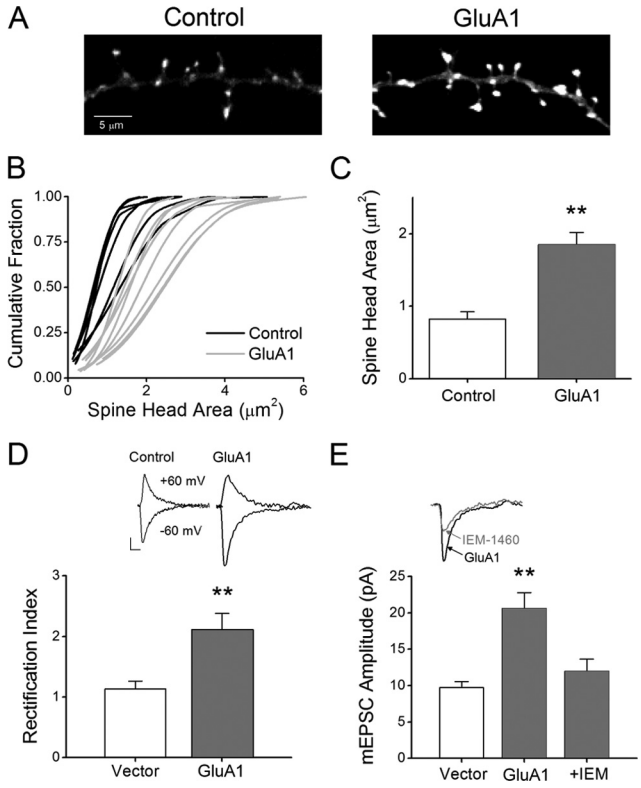

Figure 5. Overexpression of GluA1 increases spine head area, mEPSC amplitude, and synaptic expression of CP-AMPARs. ***A***, Fluorescence images of dendritic spines expressing mRFP-β-actin plus vector (left) or GluA1 (right). ***B***, Cumulative distribution plots for control neurons (black) and neurons expressing GluA1 (gray). ***C***, Mean data for neurons plotted in ***B***. Error bars indicate SEM ($n = 8$ per condition from 2 independent experiments; $^{**}p < 0.01$ by Student's *t* test). ***D***, Top, Example of mEPSCs recorded from a vector only (control) or GluA1-expressing neuron at two different holding potentials (−60 and 60 mV). Bottom, Mean rectification index, an indicator of CP-AMPARs, for vector only and GluA1 expressing neurons. Rectification index was calculated by dividing the absolute mean peak amplitude recorded at 60 mV by the peak amplitude recorded at −60 mV for individual neurons. Error bars indicate SEM ($n = 6$ recordings per condition; $^{**}p < 0.01$ by Student's *t* test). ***E***, Top, Example traces of mEPSCs recorded at −60 mV from a GluA1-expressing neuron illustrating sensitivity toward IEM-1460 (30 μM), an antagonist of CP-AMPARs. Bottom, Pooled data for mean mEPSC amplitudes for vector ($n = 6$), GluA1 ($n = 6$; $^{**}p < 0.01$ by Student's *t* test) and GluA1 in the presence of IEM-1460 (IEM; $n = 4$; $^{**}p < 0.01$ by paired Student's *t* test).

activated CaMKI is downstream of the NMDAR. Together, these data suggest that CaMKI is a relevant kinase by which NMDARs trigger activity-dependent morphological plasticity and recruitment of GluA1 to spines.

Expression of GluA1 is sufficient to drive spine expansion

It has been proposed that synaptic incorporation of the GluA1 subunit is necessary for stable increases in both spine size and synaptic strength in paradigms of NMDAR-dependent plasticity (Kopec et al., 2007). Using an antibody to the extracellular N terminus, we found that our GI-LTP paradigm resulted in a robust increase in surface GluA1 (184.4 ± 26.5% compared with control neurons) (Fig. 4*A*,*B*) that was associated with spine expansion (Fig. 4*B*, 4C). Biotinylation of receptors in nonpermeabilized cells also reflected an increase in surface GluA1 after GI-LTP induction when normalized to total GluA1 in permeabilized cells (Fig. 4*D*,*E*). This increase in surface GluA1 was dependent upon NMDARs and CaMKK as it was inhibited by APV and STO-609, respectively. Inhibition by STO-609 (Fig. 4), combined with the effects of caCaMKI (Fig. 3), suggest that CaMKK/

CaMKI regulate both surface trafficking of GluA1 into spines, as well as spine expansion after activation of synaptic NMDARs. AMPAR recruitment by GI-LTP was not specific for GluA1 as there was also an increase in surface GluA2 (supplemental Fig. S1, available at www.jneurosci.org as supplemental material).

Transfected GluA1 in cultured neurons has been shown to be incorporated into synapses as demonstrated by its punctate colocalization with surface GluA2 and an increase in current rectification (Shi et al., 1999). Therefore, we next determined whether expressing GluA1 in these neurons could mimic GI-LTP in terms of increasing spine head area. Neurons were cotransfected with wild-type GluA1 and mRFP-β-actin for 24 h before fixation, imaging, and analysis for spine head area. As shown in Figure 5*A*, expression of GluA1 led to an increase in spine head area. Cumulative probability plots illustrate that the increase in spine head area was not restricted to a subset of spines but led to a general increase in all spines measured (Fig. 5*B*). Overall, neurons expressing GluA1 demonstrated a twofold increase in spine head area (Fig. 5*C*). To confirm that the expressed GluA1 was incorporated into synapses, we performed whole-cell voltage-clamp recordings of AMPA-mediated mEPSCs at two different holding potentials (i.e., −60 and +60 mV) and measured the degree of rectification, a biophysical property associated with GluA2-lacking AMPARs (Kamboj et al., 1995). Since rectification of currents is mediated by endogenous polyamines (i.e., spermine) that can be dialyzed away during whole-cell recordings, we included spermine (100 μM) in the intracellular patch solution (Kamboj et al., 1995). We have previously demonstrated that pyramidal neuron excitatory synapses in our hippocampal cultures under basal conditions do not contain CP-AMPARs (Guire et al., 2008). However, transient expression of GluA1 likely increases the probability that GluA1 homomers will be trafficked into synapses and therefore display increased rectification. It has previously been demonstrated that the induction of NMDAR-dependent forms of synaptic plasticity results in a transient period of rectification (Plant et al., 2006; Lu et al., 2007; Guire et al., 2008). While vector only control neurons demonstrated comparable mEPSC amplitudes at both holding potentials (−60 mV = 9.7 ± 0.8 pA vs 60 mV = 8.7 ± 0.3 pA), we found that mEPSCs recorded from GluA1-expressing neurons were less conductive at positive holding potentials (−60 mV = 20.6 ± 2.2 pA vs 60 mV = 10.2 ± 1.9 pA), indicating that they were rectifying (Fig. 5*D*). To further verify the presence of CP-AMPARs, we compared the amplitude and kinetics of mEPSCs (V_h = 60 mV) in these same GluA1-expressing neurons before and after bath application of IEM-1460 (30 μM), an inhibitor of CP-AMPARs. At 30 μM, IEM-1460 inhibits only GluA2-lacking AMPARs with no effect on NMDARs (Magazanik et al., 1997; Buldakova et al., 1999; Samoilova et al., 1999; Gray et al., 2007; Guire et al., 2008). We have shown previously that IEM-1460 treatment of cultured control cells has no effect on mEPSCs, consistent with their lack of CP-AMPARs (Guire et al., 2008). Treatment of GluA1-transfected neurons with IEM-1460 resulted in a 41.9 ± 8.1% reduction in mEPSC amplitude compared with controls (Fig. 5*E*) and an increase in decay time (baseline = 5.8 ± 0.5 ms; IEM = 6.7 ± 0.5 ms; $p < 0.05$ by Student's paired t test), both properties indicative of GluA2-lacking AMPARs. Together, these data indicate that expression of GluA1 leads to synaptic incorporation of CP-AMPARs, which may drive spine expansion.

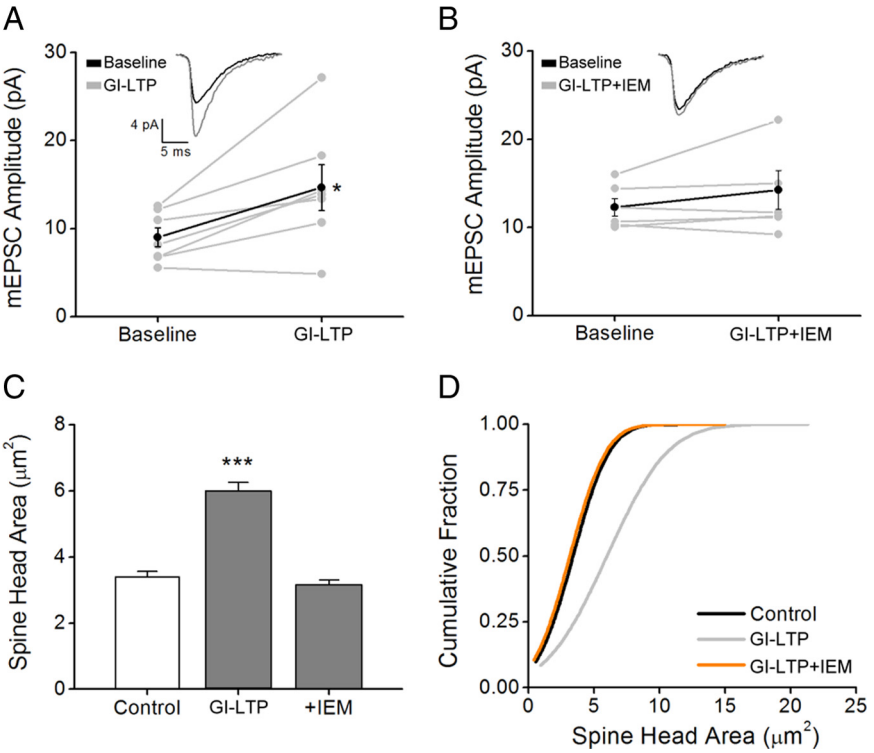

Figure 6. GI-LTP increases mEPSCs and recruitment of synaptic CP-AMPARs. ***A***, Individual mEPSC amplitudes plotted before (Baseline) and 40 min after GI-LTP. Mean amplitudes are denoted by black filled circles. Error bars indicated SEM ($n = 7$ from 3 independent cultures). *$p < 0.05$ by paired Student's t test. Inset, Example mEPSC traces before and after GI-LTP. Traces are an average of 50 consecutive events. ***B***, Plot of mEPSCs as described in ***A*** before (Baseline) and after GI-LTP in the presence of IEM-1460 (IEM). Error bars indicate SEM ($n = 6$ from 3 independent cultures). ***C***, Pooled data of spine head area ($n = 50–75$ spines per neuron; 5–8 neurons per coverslip) for controls and neurons after GI-LTP in absence or presence of IEM-1460. Error bars indicate SEM ($n = 6–8$ coverslips/ condition). ***$p < 0.001$ by Student's t test. ***D***, Cumulative distribution of spine head areas for each condition indicated.

Spine expansion induced by GI-LTP requires CP-AMPARs

To test whether GI-LTP-induced spine expansion also required CP-AMPARs, we first determined whether treatment with IEM-1460 would affect synaptic potentiation. It is well established in hippocampus that increased synaptic strength is highly associated with increases in spine volume (Cingolani and Goda, 2008). As shown in Figure 6, GI-LTP induced a 68.5 ± 9.0% increase in mEPSC amplitude (Fig. 6*A*) that was largely inhibited by coapplication of IEM-1460 (Fig. 6*B*). Importantly, we found that inhibition of CP-AMPARs during the 10 min glycine treatment also prevented the persistent spine expansion induced by GI-LTP (Fig. 6*C*,*D*). IEM-1460 had no effect on CaMKI or CaMKII activation (supplemental Fig. S3, available at www.jneurosci.org as supplemental material), indicating that IEM-1460 was not inhibiting LTP induction by nonspecifically inhibiting the activation of CaMKI or CaMKII. The fact that CaMKI activation is blocked by APV (Fig. 2) but not IEM-1460 (supplemental Fig. S3, available at www.jneurosci.org as supplemental material) indicates

the source of Ca^{2+} for its activation is dependent on NMDARs but not CP-AMPARs. This is consistent with its role in NMDAR-dependent synaptic recruitment of CP-AMPARs (Guire et al., 2008). The conclusion that IEM-1460 is acting via inhibition of AMPARs was further substantiated by the fact that application of the specific AMPAR antagonist GYKI-52466 (20 μM) also blocks spine expansion (data not shown). Interestingly, if IEM-1460 is applied after the 10 min of glycine treatment, there is still a partial suppression of spine enlargement (supplemental Fig. S4, available at www.jneurosci.org as supplemental material). These data suggest that CP-AMPARs are necessary to initiate some cellular function(s) during the glycine treatment, and this function is subsequently required for the persistent spine expansion accompanying GI-LTP. This would not be surprising if prolonged actin remodeling underlies these structural changes.

It is well established that spine structural plasticity is associated with actin polymerization (Fifkova and Delay, 1982; Matus et al., 1982; Matsuzaki et al., 2004), so we tested the effect of latrunculin A, which binds actin monomers and blocks actin polymerization. Indeed, we found that the addition of 10 μM latrunculin A prevented the spine enlargement associated with GI-LTP (Fig. 7*A*). Next, to identify the signaling pathway downstream of CP-AMPARs, we assessed the ability of GI-LTP to activate signaling molecules known to regulate the actin cytoskeleton and whether their activation was suppressed by IEM-1460. We focused on the Rac/PAK/LIMK pathway (Edwards et al., 1999) because of its known regulation of spine actin (Schubert and Dotti, 2007). To measure activation of Rac during GI-LTP, we determined the relative levels of GTP-Rac1 (i.e., active form of Rac1) by affinity pull-down using GST-tagged CRIB domain of PAK1 from control versus GI-LTP-stimulated neuronal lysates. GI-LTP resulted in a small but significant 23.5 ± 1.7% increase in Rac GTP loading normalized to total Rac protein (Fig. 7*B*). This is a significant, albeit modest, effect that may represent GTP loading of Rac only in potentiated spines (supplemental Fig. S5, available at www.jneurosci.org as supplemental material). Importantly, the GI-LTP-induced Rac1 activation was inhibited by coapplication of IEM-1460 (Fig. 7*B*). Next, we examined the activities of PAK and its downstream target LIMK using phospho-specific antibodies directed toward the activation/phosphorylation sites of PAK and LIMK (S^{141} and T^{508}, respectively). Both of these protein kinases are known regulators of the actin cytoskeleton downstream of Rac (Schubert and Dotti, 2007) and have been implicated in LTP (Allen et al., 1998; Meng et al., 2002; Hayashi et al., 2004). Consistently, we found that GI-LTP increased PAK and LIMK activation by 90.9 ± 24.4% and 153.0 ± 52.7%, respectively (Fig. 8*A*,*B*). Notably, the increase in PAK and LIMK activation after GI-LTP was dependent upon CP-AMPARs since it was inhibited by IEM-1460. In cultured hippocampal neurons, phospho-PAK has been shown to be enriched in spines as puncta that colocalize with the excitatory postsynaptic marker PSD-95 (Zhang et al., 2005). Similarly, we found an increase in phosphorylated PAK in spines after GI-LTP (supplemental Fig. S5, available at www.jneurosci.org as supplemental material), suggesting that PAK is active locally within spines. Furthermore, transfection of neurons with dnPAK (PAK^{K299R}) blocked the GI-LTP-induced spine expansion (Fig. 8*C*,*D*). Together, these data implicate a role for Rac, PAK, and its effector LIMK in the structural plasticity after the induction of GI-LTP. Of particular interest, Rac, PAK, and LIMK appear to be downstream of CP-AMPARs, providing the first functional link to a signaling pathway for CP-AMPARs in NMDA-dependent LTP.

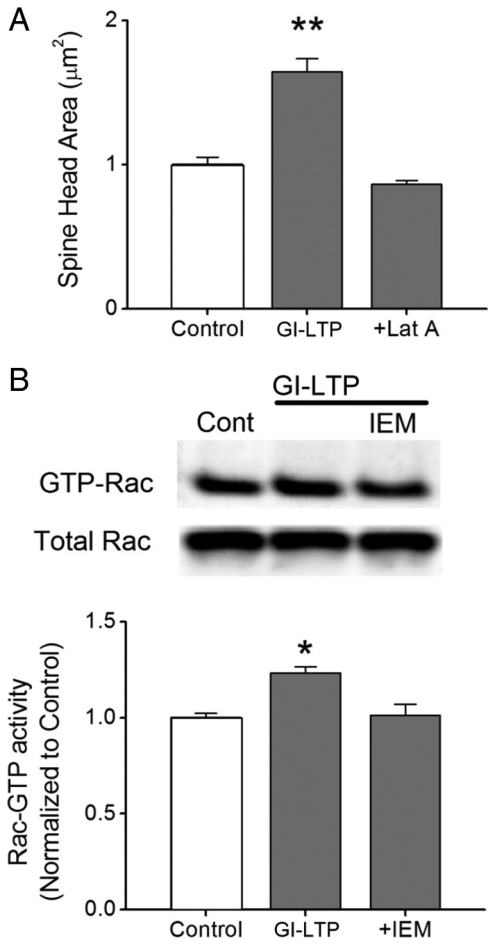

Figure 7. GI-LTP structural plasticity requires actin polymerization and CP-AMPAR-mediated activation of Rac. ***A***, Group data of spine head area ($n = 50–75$ spines per neuron; 5 neurons per coverslip) for controls and neurons subjected to GI-LTP in absence or presence of 10 μM latrunculin A. Error bars indicate SEM ($n = 5$ coverslips/condition). $^{**}p < 0.01$ by Student's *t* test. ***B***, Top, Representative Western blot of activated GTP-bound Rac, determined by affinity pulldown using GST-tagged CRIB domain of PAK1, and total Rac for conditions indicated. Bottom, Group data plotted as the ratio of GTP-Rac to total Rac for each condition normalized to the mean control. Error bars indicate SEM ($n = 4–6$ independent experiments per condition). $^{*}p < 0.05$ by Student's *t* test.

Discussion

Induction and maintenance of LTP in the CA1 region of hippocampus involves numerous biological processes including recruitment of AMPARs to synapses, phosphorylation of AMPARs, and formation and/or enlargement of spines/synapses—these require gene transcription, protein synthesis, posttranslational protein modifications, and protein trafficking (for review, see Bramham, 2008; Kerchner and Nicoll, 2008; Kessels and Malinow, 2009; Saneyoshi et al., 2010). The relative contributions of signal transduction pathways regulating these functions to the resulting synaptic potentiation may depend on the system and paradigm used to induce LTP in addition to the history of the synapse. This incredible complexity may contribute to conflicting results obtained by different investigators in this intensely investigated field.

Recent studies on activity-dependent stable enlargement of potentiated spines (i.e., structural plasticity) have focused primarily on recruitment of AMPAR subunits, particularly GluA1 and GluA2, and their associated proteins (Kopec et al., 2007; Saglietti et al., 2007). Here, we identify a novel signaling pathway

responsible for enabling stable spine enlargement after the selective activation of synaptic NMDARs in cultured hippocampal neurons. Specifically, we find a requirement for NMDAR-dependent activation of CaMKK/CaMKI-mediated synaptic expression of CP-AMPARs. These CP-AMPARs, in turn, are required for the activation of the Rac/PAK/LIMK pathway known to promote F-actin polymerization in spines. Our conclusions are based on multiple, independent experimental approaches. These results are consistent with our previous report that although expressed on the cell surface of dendrites, CP-AMPARs are not present within the synapse under basal conditions (Guire et al., 2008). Importantly, infusion of activated CaMKI alone in cultured neurons drives CP-AMPARs into the synapse and increases synaptic strength. Here, we report that transfection of caCaMKI in cultured hippocampal neurons increases the surface expression of GluA1 in spines and promotes stable spine enlargement. Furthermore, induction of TBS LTP in the CA1 region of hippocampal slices results in a partial (~50%) contribution by CP-AMPARs to the synaptic potentiation. However, the contribution of CP-AMPARs to LTP induced by other protocols [e.g., high-frequency stimulation (HFS) or paired presynaptic/postsynaptic stimulation] remains controversial (Adesnik and Nicoll, 2007; Gray et al., 2007).

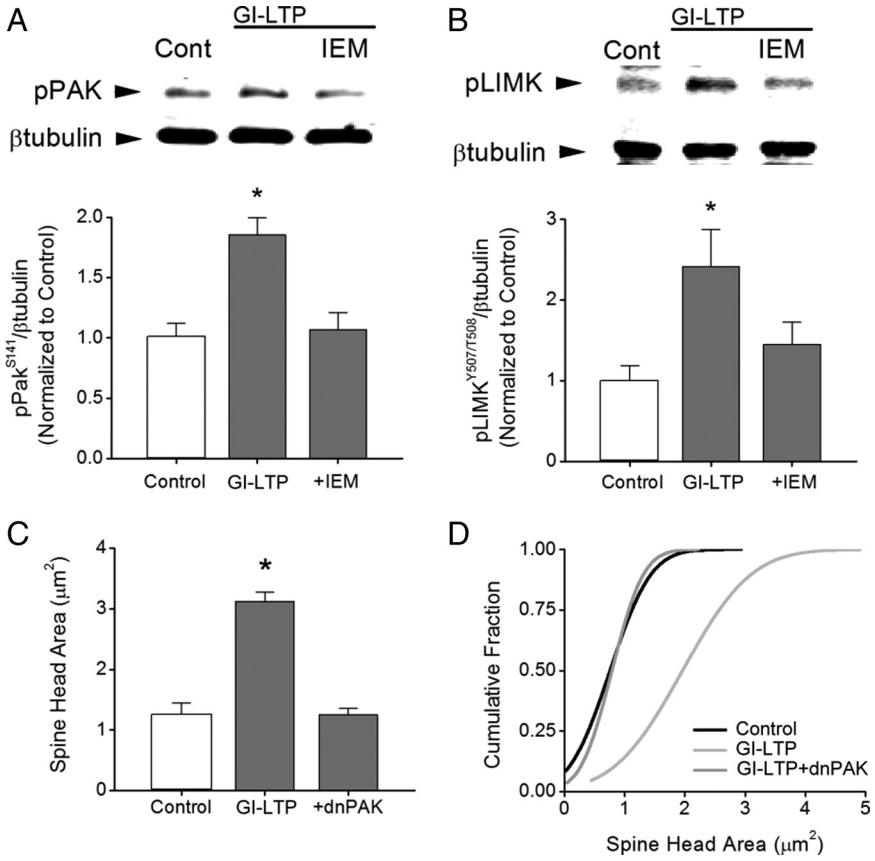

Figure 8. GI-LTP structural plasticity requires the PAK/LIM-kinase Pathway. ***A***, Top, Western blots of pPAK (S141) and β-tubulin (loading control) for conditions indicated. Bottom, Group data shown as the ratio of pPAK to β-tubulin for each condition normalized to the mean control. ***B***, Top, In these same experiments cell lysates were also probed by Western blots for pLIMK (Y507/T508). Bottom, Pooled data for ratios of pLIMK to β-tubulin for each condition normalized to the mean control. Error bars in ***A*** and ***B*** indicate SEM ($n = 6–7$ independent experiments). *$p < 0.05$ by Student's *t* test. ***C***, Mean spine head area for control and neurons after GI-LTP treatment in the absence or presence of dnPAK ($n = 50–75$ spines per neuron; 5–6 neurons per coverslip). Error bars indicate SEM ($n = 8–10$ coverslips per condition from 2–3 independent cultures). *$p < 0.05$ by Student's *t* test. ***D***, Cumulative distribution of spine head areas for each condition indicated.

Roles for CP-AMPARs in synaptic plasticity are well established at interneuron synapses (Liu and Zukin, 2007). For example, in the spinal cord synaptic potentiation mediated by CP-AMPARs expressed by GABA-containing interneurons in the dorsal horn contributes to chronic pain (Gu et al., 1996; Hartmann et al., 2004). In contrast, HFS of mossy fiber synapses onto CA3 interneurons induces LTD via CP-AMPARs (Laezza et al., 1999; Lei and McBain, 2004). Surprisingly, very little was previously known about detailed signaling pathways downstream of these unique receptors. In cultured mouse striatal neurons, activation of CP-AMPARs results in stimulation of phosphatidylinositol 3-kinase, MEK/Erk, and CREB phosphorylation (Perkinton et al., 1999). In mature cortical neurons and slices, CP-AMPARs form a complex with the Ca^{2+}/CaM-activated Ras/Rac GEF, Ras-GRF1, that is predominantly responsible for Erk activation and CREB phosphorylation (Tian and Feig, 2006). However, in postpubescent mice Ras-GRF1 appears to mediate NMDAR-dependent LTD rather than LTP (Li et al., 2006). It should be noted that the CaMKK/CaMKI pathway can also active the MEK/Erk pathway (Schmitt et al., 2004) resulting in CREB-dependent transcription (Wayman et al., 2006). Furthermore, phosphorylation of Ras-GRF1 (Ser^{916}) upon LTP induction is blocked by inhibitors of CaMKK (Schmitt et al., 2005), implicating that Ras-GRF1 may be downstream of CaMKK.

It is well documented that increased spine size during LTP requires regulation of the actin cytoskeleton (for review, see Matus, 2000; Hering and Sheng, 2001; Carlisle and Kennedy, 2005; Tada and Sheng, 2006), so we focused on signaling pathways known to regulate actin dynamics. Our results are the first to provide a mechanism by which CP-AMPARs can contribute to synaptic potentiation at excitatory CA1 synapses via spine enlargement through activation of the Rac/PAK/LIMK pathway that regulates the actin cytoskeleton. These results are consistent with previous reports indicating a role for PAK in activity-dependent alterations of spine enlargement (Chen et al., 2007; Rex et al., 2009). Importantly, mutations in PAK have been found in patients with nonsyndromic mental retardation, indicating their importance in cognitive function (Allen et al., 1998; Bienvenu et al., 2000). LIMK is a well established downstream effector of PAK that enhances formation of F-actin (Edwards et al., 1999) and is also involved in LTP (Meng et al., 2002).

Our results identify an important role for recruitment of the GluA1 subunit of AMPARs to form synaptic CP-AMPARs contributing to stable structural plasticity. Previous studies have identified roles for both the GluA1 and GluA2 subunits. In cultured neurons (22 DIV), expression of GluA2 promotes spine enlargement via interaction of its N-terminus with N-cadherin (Saglietti et al., 2007). Although we focused on the role of GluA1, our GI-LTP protocol also increases surface expression of GluA2 (supplemental Fig. S1, available at www.jneurosci.org as supple-

mental material) that may also contribute to the spine enlargement in our experiments. In contrast to our study, Saglietti et al. did not see any effect of expressing GluA1 on spine size. Although expressed GluA1 in cultured neurons is generally trafficked to the synapse (Shi et al., 1999), this was not actually determined in the Saglietti study. Whether expressed GluA1 is incorporated into synapses may depend on the extent of endogenous neuronal activity present and/or the activation state of CaMKs. In organotypic slices, transiently transfected GluA1 is not localized to synapses unless coexpressed with active CaMKII or the slice is stimulated (Hayashi et al., 2000). Our experience, based on recordings of mEPSCs and measuring the activation states of CaMKII and CaMKI, is that mature cultures of hippocampal neurons exhibit higher levels of endogenous activity than do acute or cultured hippocampal slices (unpublished observations). Thus, the level of endogenous activity in cultured neurons may dictate whether expressed GluA1 is trafficked to synapses.

Several studies have implicated roles for the GluA1 subunit in increasing synaptic strength associated with LTP (for review, see Barry and Ziff, 2002; see Kopec et al., 2007; Makino and Malinow, 2009). One study, using organotypic hippocampal slices, identified the C terminus of GluA1, which contains an essential PDZ interaction site as well as multiple phosphorylation sites, as the essential domain for spine expansion (Kopec et al., 2007). Surprisingly, they found that expression of GluA1 with a mutation in the pore that obviates channel permeation still promotes increased spine size. However, we find that activity-dependent blockade of CP-AMPARS by IEM-1460 suppresses spine enlargement induced by GI-LTP. Kopec et al. (2007) note, "Although our study argues against a requirement for calcium entry through GluA2-lacking AMPA receptors, it may be that our LTP induction protocol, which is 16 min long, provides ample Ca^{2+} influx through NMDA receptors to both drive GluA1 receptors into synapses and subsequently stabilize them there." Their c-LTP treatment protocol of forskolin/rolipram gives synaptic potentiation that mimics standard strong (e.g., HFS) LTP protocols (Otmakhov et al., 2004), and it results in global activation of PKA throughout the neuron including presynaptic and postsynaptic compartments. In our study, we took advantage of a GI-LTP protocol that requires spontaneous release of glutamate from opposing terminals to specifically activate postsynaptic NMDARs and CaMKs.

In the same report Kopec et al. (2007) showed that spine enlargement precedes by several minutes the recruitment of AMPARs. This would appear to be at odds with our results where synaptic incorporation of CP-AMPARs was required for spine expansion. Since overexpression of GluA1 was sufficient by itself to promote spine enlargement that was blocked by IEM-1460, our data strongly indicate that recruitment of some CP-AMPARs is required before structural plasticity. Due to the unique properties of CP-AMPARS (e.g., high unitary conductance, stabilization in high-conductance state by CaMKII phosphorylation), only a very small number (<5% of total synaptic AMPARs) (Guire et al., 2008) need be recruited to the synapse to have a large effect on synaptic current and the Ca^{2+} influx that may be required for triggering the Rac/PAK/LIMK pathway. This very small number of CP-AMPARs would not be detectable by most methods used to quantify GluA1 trafficking. Thus, there may be initial recruitment of a small number of synaptic CP-AMPARs that precedes and triggers spine expansion followed by a subsequent bulk recruitment of AMPARs (perhaps GluA1/GluA2) that stabilizes the enlarged spine.

Previous studies have provided evidence for roles of the CaMKK/CaMKI pathway in numerous aspects of neuronal development, such as axon formation (Ageta-Ishihara et al., 2009; Davare et al., 2009) and outgrowth (Wayman et al., 2004), dendritic arborization (Wayman et al., 2006), and spine/synapses formation (Saneyoshi et al., 2008), as well contributing to TBS LTP (Schmitt et al., 2005) through recruitment of CP-AMPARs (Guire et al., 2008). The current study adds to this list of neuronal functions, namely, spine enlargement in mature neurons during NMDAR-dependent structural plasticity, regulated by CaMKK/CaMKI. Specifically, we demonstrate that GI-LTP, via NMDAR activation of CaMKK/CaMKI, promotes synaptic expression of CP-AMPARs. CP-AMPARs have not previously been implicated in promoting spine enlargement, and this may account for the role of CP-AMPARs in TBS LTP (Guire et al., 2008). Furthermore, our results establish an essential role for CP-AMPARs in the activation of the Rac/PAK/LIMK pathway essential for modulating activity-dependent actin dynamics within hippocampal dendritic spines.

References

Abramoff MD, Magelhaes PJ, Ram SJ (2004) Image processing with ImageJ. Biophotonics Int 11:36–42.

Adesnik H, Nicoll RA (2007) Conservation of glutamate receptor 2-containing AMPA receptors during long-term potentiation. J Neurosci 27:4598–4602.

Ageta-Ishihara N, Takemoto-Kimura S, Nonaka M, Adachi-Morishima A, Suzuki K, Kamijo S, Fujii H, Mano T, Blaeser F, Chatila TA, Mizuno H, Hirano T, Tagawa Y, Okuno H, Bito H (2009) Control of cortical axon elongation by a GABA-driven Ca^{2+}/calmodulin-dependent protein kinase cascade. J Neurosci 29:13720–13729.

Allen KM, Gleeson JG, Bagrodia S, Partington MW, MacMillan JC, Cerione RA, Mulley JC, Walsh CA (1998) PAK3 mutation in nonsyndromic X-linked mental retardation. Nat Genet 20:25–30.

Bamburg JR, McGough A, Ono S (1999) Putting a new twist on actin: ADF/cofilins modulate actin dynamics. Trends Cell Biol 9:364–370.

Barry MF, Ziff EB (2002) Receptor trafficking and the plasticity of excitatory synapses. Curr Opin Neurobiol 12:279–286.

Bienvenu T, des Portes V, McDonell N, Carrié A, Zemni R, Couvert P, Ropers HH, Moraine C, van Bokhoven H, Fryns JP, Allen K, Walsh CA, Boué J, Kahn A, Chelly J, Beldjord C (2000) Missense mutation in PAK3, R67C, causes X-linked nonspecific mental retardation. Am J Med Genet 93:294–298.

Boda B, Nikonenko I, Alberi S, Muller D (2006) Central nervous system functions of PAK protein family: from spine morphogenesis to mental retardation. Mol Neurobiol 34:67–80.

Bourne JN, Harris KM (2008) Balancing structure and function at hippocampal dendritic spines. Annu Rev Neurosci 31:47–67.

Bramham CR (2008) Local protein synthesis, actin dynamics, and LTP consolidation. Curr Opin Neurobiol 18:524–531.

Buldakova SL, Vorobjev VS, Sharonova IN, Samoilova MV, Magazanik LG (1999) Characterization of AMPA receptor populations in rat brain cells by the use of subunit-specific open channel blocking drug, IEM-1460. Brain Res 846:52–58.

Carlisle HJ, Kennedy MB (2005) Spine architecture and synaptic plasticity. Trends Neurosci 28:182–187.

Chang BH, Mukherji S, Soderling TR (1998) Characterization of a calmodulin kinase II inhibitor protein in brain. Proc Natl Acad Sci U S A 95:10890–10895.

Chang BH, Mukherji S, Soderling TR (2001) Calcium/calmodulin-dependent protein kinase II inhibitor protein: localization of isoforms in rat brain. Neuroscience 102:767–777.

Chen LY, Rex CS, Casale MS, Gall CM, Lynch G (2007) Changes in synaptic morphology accompany actin signaling during LTP. J Neurosci 27:5363–5372.

Cingolani LA, Goda Y (2008) Actin in action: the interplay between the actin cytoskeleton and synaptic efficacy. Nat Rev Neurosci 9:344–356.

Davare MA, Saneyoshi T, Guire ES, Nygaard SC, Soderling TR (2004) Inhibition of calcium/calmodulin-dependent protein kinase kinase by protein 14–3-3. J Biol Chem 279:52191–52199.

Davare MA, Fortin DA, Saneyoshi T, Nygaard S, Kaech S, Banker G, Soderling TR, Wayman GA (2009) Transient receptor potential canonical 5 channels activate Ca^{2+}/calmodulin kinase Igamma to promote axon formation in hippocampal neurons. J Neurosci 29:9794–9808.

Edwards DC, Sanders LC, Bokoch GM, Gill GN (1999) Activation of LIM-kinase by Pak1 couples Rac/Cdc42 GTPase signalling to actin cytoskeletal dynamics. Nat Cell Biol 1:253–259.

Fiala JC, Spacek J, Harris KM (2002) Dendritic spine pathology: cause or consequence of neurological disorders? Brain Res Brain Res Rev 39:29–54.

Fifková E (1985) A possible mechanism of morphometric changes in dendritic spines induced by stimulation. Cell Mol Neurobiol 5:47–63.

Fifková E, Delay RJ (1982) Cytoplasmic actin in neuronal processes as a possible mediator of synaptic plasticity. J Cell Biol 95:345–350.

Gray EE, Fink AE, Sariñana J, Vissel B, O'Dell TJ (2007) Long-term potentiation in the hippocampal CA1 region does not require insertion and activation of GluR2-lacking AMPA receptors. J Neurophysiol 98:2488–2492.

Gu JG, Albuquerque C, Lee CJ, MacDermott AB (1996) Synaptic strengthening through activation of Ca2+-permeable AMPA receptors. Nature 381:793–796.

Guire ES, Oh MC, Soderling TR, Derkach VA (2008) Recruitment of calcium-permeable AMPA receptors during synaptic potentiation is regulated by CaM-kinase I. J Neurosci 28:6000–6009.

Hartmann B, Ahmadi S, Heppenstall PA, Lewin GR, Schott C, Borchardt T, Seeburg PH, Zeilhofer HU, Sprengel R, Kuner R (2004) The AMPA receptor subunits GluR-A and GluR-B reciprocally modulate spinal synaptic plasticity and inflammatory pain. Neuron 44:637–650.

Hayashi K, Ohshima T, Hashimoto M, Mikoshiba K (2007) Pak1 regulates dendritic branching and spine formation. Dev Neurobiol 67:655–669.

Hayashi ML, Choi SY, Rao BS, Jung HY, Lee HK, Zhang D, Chattarji S, Kirkwood A, Tonegawa S (2004) Altered cortical synaptic morphology and impaired memory consolidation in forebrain- specific dominant-negative PAK transgenic mice. Neuron 42:773–787.

Hayashi Y, Shi SH, Esteban JA, Piccini A, Poncer JC, Malinow R (2000) Driving AMPA receptors into synapses by LTP and CaMKII: requirement for GluR1 and PDZ domain interaction. Science 287:2262–2267.

Hebb DO (1949) Organisation of behaviour. New York: Wiley.

Hering H, Sheng M (2001) Dendritic spines: structure, dynamics and regulation. Nat Rev Neurosci 2:880–888.

Impey S, Davare M, Lasiek A, Fortin D, Ando H, Varlamova O, Obrietan K, Soderling TR, Goodman RH, Wayman GA (2010) An activity-induced microRNA controls dendritic spine formation by regulating Rac1-PAK signaling. Mol Cell Neurosci 43:146–156.

Kamboj SK, Swanson GT, Cull-Candy SG (1995) Intracellular spermine confers rectification on rat calcium-permeable AMPA and kainate receptors. J Physiol 486:297–303.

Kaufmann WE, Moser HW (2000) Dendritic anomalies in disorders associated with mental retardation. Cereb Cortex 10:981–991.

Kerchner GA, Nicoll RA (2008) Silent synapses and the emergence of a postsynaptic mechanism for LTP. Nat Rev Neurosci 9:813–825.

Kessels HW, Malinow R (2009) Synaptic AMPA receptor plasticity and behavior. Neuron 61:340–350.

Kopec CD, Real E, Kessels HW, Malinow R (2007) GluR1 links structural and functional plasticity at excitatory synapses. J Neurosci 27:13706–13718.

Korkotian E, Segal M (2007) Morphological constraints on calcium dependent glutamate receptor trafficking into individual dendritic spine. Cell Calcium 42:41–57.

Laezza F, Doherty JJ, Dingledine R (1999) Long-term depression in hippocampal interneurons: joint requirement for pre- and postsynaptic events. Science 285:1411–1414.

Lei S, McBain CJ (2004) Two Loci of expression for long-term depression at hippocampal mossy fiber-interneuron synapses. J Neurosci 24:2112–2121.

Li S, Tian X, Hartley DM, Feig LA (2006) The environment versus genetics in controlling the contribution of MAP kinases to synaptic plasticity. Curr Biol 16:2303–2313.

Liu SJ, Zukin RS (2007) Ca2+-permeable AMPA receptors in synaptic plasticity and neuronal death. Trends Neurosci 30:126–134.

Lu W, Man H, Ju W, Trimble WS, MacDonald JF, Wang YT (2001) Activation of synaptic NMDA receptors induces membrane insertion of new AMPA receptors and LTP in cultured hippocampal neurons. Neuron 29:243–254.

Lu Y, Allen M, Halt AR, Weisenhaus M, Dallapiazza RF, Hall DD, Usachev YM, McKnight GS, Hell JW (2007) Age-dependent requirement of AKAP150-anchored PKA and GluR2-lacking AMPA receptors in LTP. EMBO J 26:4879–4890.

Magazanik LG, Buldakova SL, Samoilova MV, Gmiro VE, Mellor IR, Usherwood PN (1997) Block of open channels of recombinant AMPA receptors and native AMPA/kainate receptors by adamantane derivatives. J Physiol 505:655–663.

Makino H, Malinow R (2009) AMPA receptor incorporation into synapses during LTP: the role of lateral movement and exocytosis. Neuron 64:381–390.

Matsuzaki M, Honkura N, Ellis-Davies GC, Kasai H (2004) Structural basis of long-term potentiation in single dendritic spines. Nature 429:761–766.

Matus A (2000) Actin-based plasticity in dendritic spines. Science 290:754–758.

Matus A, Ackermann M, Pehling G, Byers HR, Fujiwara K (1982) High actin concentrations in brain dendritic spines and postsynaptic densities. Proc Natl Acad Sci U S A 79:7590–7594.

Meng Y, Zhang Y, Tregoubov V, Janus C, Cruz L, Jackson M, Lu WY, MacDonald JF, Wang JY, Falls DL, Jia Z (2002) Abnormal spine morphology and enhanced LTP in LIMK-1 knockout mice. Neuron 35:121–133.

Oertner TG, Matus A (2005) Calcium regulation of actin dynamics in dendritic spines. Cell Calcium 37:477–482.

Oh MC, Derkach VA (2005) Dominant role of the GluR2 subunit in regulation of AMPA receptors by CaMKII. Nat Neurosci 8:853–854.

Oh MC, Derkach VA, Guire ES, Soderling TR (2006) Extrasynaptic membrane trafficking regulated by GluR1 serine 845 phosphorylation primes AMPA receptors for long-term potentiation. J Biol Chem 281:752–758.

Otmakhov N, Khibnik L, Otmakhova N, Carpenter S, Riahi S, Asrican B, Lisman J (2004) Forskolin-induced LTP in the CA1 hippocampal region is NMDA receptor dependent. J Neurophysiol 91:1955–1962.

Ovtscharoff W Jr, Segal M, Goldin M, Helmeke C, Kreher U, Greenberger V, Herzog A, Michaelis B, Braun K (2008) Electron microscopic 3D-reconstruction of dendritic spines in cultured hippocampal neurons undergoing synaptic plasticity. Dev Neurobiol 68:870–876.

Park M, Salgado JM, Ostroff L, Helton TD, Robinson CG, Harris KM, Ehlers MD (2006) Plasticity-induced growth of dendritic spines by exocytic trafficking from recycling endosomes. Neuron 52:817–830.

Penzes P, Beeser A, Chernoff J, Schiller MR, Eipper BA, Mains RE, Huganir RL (2003) Rapid induction of dendritic spine morphogenesis by trans-synaptic ephrinB-EphB receptor activation of the Rho-GEF kalirin. Neuron 37:263–274.

Perkinton MS, Sihra TS, Williams RJ (1999) Ca^{2+}-permeable AMPA receptors induce phosphorylation of cAMP response element-binding protein through a phosphatidylinositol 3-kinase-dependent stimulation of the mitogen-activated protein kinase signaling cascade in neurons. J Neurosci 19:5861–5874.

Pickard L, Noël J, Duckworth JK, Fitzjohn SM, Henley JM, Collingridge GL, Molnar E (2001) Transient synaptic activation of NMDA receptors leads to the insertion of native AMPA receptors at hippocampal neuronal plasma membranes. Neuropharmacology 41:700–713.

Plant K, Pelkey KA, Bortolotto ZA, Morita D, Terashima A, McBain CJ, Collingridge GL, Isaac JT (2006) Transient incorporation of native GluR2-lacking AMPA receptors during hippocampal long-term potentiation. Nat Neurosci 9:602–604.

Purpura DP (1974) Dendritic spine "dysgenesis" and mental retardation. Science 186:1126–1128.

Ramón y Cajal S (1911) Histologie du systeme nerveux de l'homme et des vertbres. Paris: Maloine.

Rex CS, Chen LY, Sharma A, Liu J, Babayan AH, Gall CM, Lynch G (2009) Different Rho GTPase-dependent signaling pathways initiate sequential steps in the consolidation of long-term potentiation. J Cell Biol 186:85–97.

Saglietti L, Dequidt C, Kamieniarz K, Rousset MC, Valnegri P, Thoumine O, Beretta F, Fagni L, Choquet D, Sala C, Sheng M, Passafaro M (2007) Extracellular interactions between GluR2 and N-cadherin in spine regulation. Neuron 54:461–477.

Samoilova MV, Buldakova SL, Vorobjev VS, Sharonova IN, Magazanik LG (1999) The open channel blocking drug, IEM-1460, reveals functionally

distinct alpha-amino-3-hydroxy-5-methyl-4-isoxazolepropionate receptors in rat brain neurons. Neuroscience 94:261–268.

Saneyoshi T, Wayman G, Fortin D, Davare M, Hoshi N, Nozaki N, Natsume T, Soderling TR (2008) Activity-dependent synaptogenesis: regulation by a CaM-kinase kinase/CaM-kinase I/betaPIX signaling complex. Neuron 57:94–107.

Saneyoshi T, Fortin DA, Soderling TR (2010) Regulation of spine and synapse formation by activity-dependent intracellular signaling pathways. Curr Opin Neurobiol 20:108–115.

Schmitt JM, Wayman GA, Nozaki N, Soderling TR (2004) Calcium activation of ERK mediated by calmodulin kinase I. J Biol Chem 279: 24064–24072.

Schmitt JM, Guire ES, Saneyoshi T, Soderling TR (2005) Calmodulin-dependent kinase kinase/calmodulin kinase I activity gates extracellular-regulated kinase-dependent long-term potentiation. J Neurosci 25:1281–1290.

Schubert V, Dotti CG (2007) Transmitting on actin: synaptic control of dendritic architecture. J Cell Sci 120:205–212.

Shahi K, Baudry M (1993) Glycine-induced changes in synaptic efficacy in hippocampal slices involve changes in AMPA receptors. Brain Res 627:261–266.

Shi SH, Hayashi Y, Petralia RS, Zaman SH, Wenthold RJ, Svoboda K, Malinow R (1999) Rapid spine delivery and redistribution of AMPA receptors after synaptic NMDA receptor activation. Science 284:1811–1816.

Shi S, Hayashi Y, Esteban JA, Malinow R (2001) Subunit-specific rules governing AMPA receptor trafficking to synapses in hippocampal pyramidal neurons. Cell 105:331–343.

Silva AJ, Stevens CF, Tonegawa S, Wang Y (1992) Deficient hippocampal long-term potentiation in alpha-calcium-calmodulin kinase II mutant mice. Science 257:201–206.

Steiner P, Higley MJ, Xu W, Czervionke BL, Malenka RC, Sabatini BL (2008) Destabilization of the postsynaptic density by PSD-95 serine 73 phosphorylation inhibits spine growth and synaptic plasticity. Neuron 60:788–802.

Tada T, Sheng M (2006) Molecular mechanisms of dendritic spine morphogenesis. Curr Opin Neurobiol 16:95–101.

Tassabehji M, Metcalfe K, Fergusson WD, Carette MJ, Dore JK, Donnai D, Read AP, Pröschel C, Gutowski NJ, Mao X, Sheer D (1996) LIM-kinase deleted in Williams syndrome. Nat Genet 13:272–273.

Tian X, Feig LA (2006) Age-dependent participation of Ras-GRF proteins in coupling calcium-permeable AMPA glutamate receptors to Ras/Erk signaling in cortical neurons. J Biol Chem 281:7578–7582.

Tokumitsu H, Enslen H, Soderling TR (1995) Characterization of a Ca2+/calmodulin-dependent protein kinase cascade. Molecular cloning and expression of calcium/calmodulin-dependent protein kinase kinase. J Biol Chem 270:19320–19324.

Tokumitsu H, Inuzuka H, Ishikawa Y, Ikeda M, Saji I, Kobayashi R (2002) STO-609, a specific inhibitor of the Ca(2+)/calmodulin-dependent protein kinase kinase. J Biol Chem 277:15813–15818.

Tokumitsu H, Inuzuka H, Ishikawa Y, Kobayashi R (2003) A single amino acid difference between alpha and beta Ca2+/calmodulin-dependent protein kinase kinase dictates sensitivity to the specific inhibitor, STO-609. J Biol Chem 278:10908–10913.

Vlachos A, Korkotian E, Schonfeld E, Copanaki E, Deller T, Segal M (2009) Synaptopodin regulates plasticity of dendritic spines in hippocampal neurons. J Neurosci 29:1017–1033.

Wayman GA, Kaech S, Grant WF, Davare M, Impey S, Tokumitsu H, Nozaki N, Banker G, Soderling TR (2004) Regulation of axonal extension and growth cone motility by calmodulin-dependent protein kinase I. J Neurosci 24:3786–3794.

Wayman GA, Impey S, Marks D, Saneyoshi T, Grant WF, Derkach V, Soderling TR (2006) Activity-dependent dendritic arborization mediated by CaM-kinase I activation and enhanced CREB-dependent transcription of Wnt-2. Neuron 50:897–909.

Zhang H, Webb DJ, Asmussen H, Niu S, Horwitz AF (2005) A GIT1/PIX/Rac/PAK signaling module regulates spine morphogenesis and synapse formation through MLC. J Neurosci 25:3379–3388.